Annals of Anatomy 203 (2016) 59–68

Contents lists available at ScienceDirect

Annals of Anatomy

journal homepage: www.elsevier.com/locate/aanat

The relationship between skull morphology, masticatory muscle force and cranial skeletal deformation during biting☆

Viviana Toro-Ibacache[a,b,c,*], Víctor Zapata Muñoz[d], Paul O'Higgins[a]

[a] Department of Archaeology and Hull York Medical School, University of York, Heslington, York YO10 5DD, United Kingdom
[b] Facultad de Odontología, Universidad de Chile, Sergio Livingstone Pohlhammer 943, Independencia, Región Metropolitana, Chile
[c] Max Planck Institute for Evolutionary Anthropology, Department of Human Evolution, Deutscher Platz 6, 04103 Leipzig, Germany
[d] Centro de Imagenología, Hospital Clínico Universidad de Chile, Santos Dumont 999, Independencia, Región Metropolitana, Chile

ARTICLE INFO

Article history:
Received 28 November 2014
Received in revised form 27 February 2015
Accepted 1 March 2015

Keywords:
Modern humans
Skull morphology
Masticatory function
Geometric morphometrics
Finite element analysis

ABSTRACT

The human skull is gracile when compared to many Middle Pleistocene hominins. It has been argued that it is less able to generate and withstand high masticatory forces, and that the morphology of the lower portion of the modern human face correlates most strongly with dietary characteristics. This study uses geometric morphometrics and finite element analysis (FEA) to assess the relationship between skull morphology, muscle force and cranial deformations arising from biting, which is relevant in understanding how skull morphology relates to mastication. The three-dimensional skull anatomies of 20 individuals were reconstructed from medical computed tomograms. Maximal contractile muscle forces were estimated from muscular anatomical cross-sectional areas (CSAs). Fifty-nine landmarks were used to represent skull morphology. A partial least squares analysis was performed to assess the association between skull shape and muscle force, and FEA was used to compare the deformation (strains) generated during incisor and molar bites in two individuals representing extremes of morphological variation in the sample. The results showed that only the proportion of total muscle CSA accounted for by the temporalis appears associated with skull morphology, albeit weekly. However, individuals with a large temporalis tend to possess a relatively wider face, a narrower, more vertically oriented maxilla and a lower positioning of the coronoid process. The FEAs showed that, despite differences in morphology, biting results in similar modes of deformation for both crania, but with localised lower magnitudes of strains arising in the individual with the narrowest, most vertically oriented maxilla. Our results suggest that the morphology of the maxilla modulates the transmission of forces generated during mastication to the rest of the cranium by deforming less in individuals with the ability to generate proportionately larger temporalis muscle forces.

1. Introduction

The relationship between masticatory function and skull form is key to understanding the functional determinants of phenotypic evolution (Demes, 1987; Spencer and Demes, 1993; Antón, 1996; O'Connor et al., 2005) and development (Anderson et al., 2014; Kiliaridis et al., 1989). Some authors have found a relationship between dietary ecology and metric traits of the skull (Dumont, 1997; Muchlinski and Deane, 2014; Taylor, 2006) in non-human primates, whereas in modern humans it has been suggested that the relationship is most strongly localised to the mandible (von Cramon-Taubadel, 2011) or it is obscured by other variables such as population history and geography (González-José et al., 2005; Menéndez et al., 2014). Thus, the extent to which a genetically determined phenotype can be modified by function, and when this modification translates into a functionally adapted phenotype remains unknown.

Muscle forces and skeletal morphology are linked through the process of bone remodelling. During contraction, muscles directly strain the bone where they insert and apply loads. They also impact on strains elsewhere during loading (DiGirolamo et al., 2013; Milne and O'Higgins, 2012; Moss, 1962; Ross and Iriarte-Diaz, 2014; Scott, 1957; Yoshikawa et al., 1994). Excessive bone strains derived from loadings or diminished strains induce or reduce the amount and

☆ Grant sponsor: Corporación Nacional Científica Tecnológica (Chile). Grant: Becas Chile awarded to Viviana Toro-Ibacache.

* Corresponding author at: Max Planck Institute for Evolutionary Anthropology, Department of Human Evolution, Deutscher Platz 6, 04103 Leipzig, Germany. Tel.: +49 341 3550 870.
E-mail address: mtoroibacache@odontologia.uchile.cl (V. Toro-Ibacache).

http://dx.doi.org/10.1016/j.aanat.2015.03.002
0940-9602/

direction of bone formation and resorption, changing bone morphology (Barak et al., 2011; Rubin and Lanyon, 1985) in such a way that the new form responds to the loads by developing strains that lie within the range of bone mass maintenance (Frost, 1987) and functional optimisation (i.e., maximal strength with minimal material; Ross and Metzger, 2004). Mechanical models of the human masticatory system (Gingerich, 1979; Hylander, 1975; Koolstra et al., 1988; Röhrle and Pullan, 2007; Spencer, 1998) have shown that jaw-elevator muscles play a key role in the generation of reaction force at the temporomandibular joints (TMJs) and in influencing the magnitudes of bite forces (Sellers and Crompton, 2004). The same studies demonstrated that, because of lever mechanics, forces produced during mastication are also influenced by anatomical features such as the relative positions of the TMJs, muscle insertions and dental morphology.

It has been shown in macaques that individuals with longer mandibular bodies have larger physiological cross-sectional areas (PCSAs), which relate to muscle forces (Koolstra et al., 1988; O'Connor et al., 2005; Weijs and Hillen, 1985). This has been interpreted as an adaptation that maintains bite forces; when the bite force lever arms increase, muscle forces also increase (Antón, 1999). The same relationship has also been found in humans using muscle cross sectional area (CSA) (Hannam and Wood, 1989; Weijs and Hillen, 1986). CSA, rather than PCSA of human masticatory muscles is often used to estimate muscle force because it can be directly measured in computed tomographic or magnetic resonance images and has been shown to correlate with PCSA (Hannam and Wood, 1989; van Spronsen et al., 1992; Weijs and Hillen, 1986). Significant correlations have also been found between measures of facial width and the CSA of the medial pterygoid (Hannam and Wood, 1989; van Spronsen et al., 1992), the temporalis muscle and most markedly, the masseter muscles (Hannam and Wood, 1989; Raadsheer et al., 1999; van Spronsen et al., 1991, 1992; Weijs and Hillen, 1986).

The above-mentioned studies evaluated skull morphology using linear morphometrics. New geometric morphometric tools have been developed over the last three decades (Rohlf and Marcus, 1993; O'Higgins and Jones, 1998; Slice, 2007) for studying shape variation and its causes. Geometric morphometrics facilitates visualisation of the results of statistical analyses as warpings of surface models. In the present study we use such an approach to quantify and characterise the relationship between skull shape and muscle force (estimated via CSA). In addition, we use a second approach, finite element analysis (FEA) to predict cranial deformation under simulated biting loads. This technique has been increasingly used to study the response of the skull to masticatory loading in terms of the stresses and/or strains developed in the skeleton, relating these to ecological (Macho et al., 2005; Strait et al., 2009), anatomo-functional (Koolstra and Tanaka, 2009; Ross et al., 2011), evolutionary (Gröning et al., 2011; Wroe et al., 2010) and developmental factors (Kupczik et al., 2009). FEA is used in the present study to characterise the deformations of the cranium that arise in response to biting in two individuals representing the extremes of cranial variation in our available sample.

The following null hypotheses are tested:

Hypothesis 1 (H01). There is no association between skull shape and the CSAs of masticatory muscles.

This hypothesis is tested using geometric morphometric analyses to examine the associations between CSAs and cranial form.

Hypothesis 2 (H02). Crania with different morphologies show different modes of deformation in response to identical biting loads.

H02 will be tested using FEA in order to assess the modes and magnitudes of cranial deformation in two individuals representing the extremes of variation by comparing the distributions (i.e., spatial patterning of high and low values), and magnitudes of strains.

2. Material and methods

The computed tomograms (CTs) of 20 adult humans, 11 female (aged 29–86 years) and 9 male (aged 38–72 years) were used in this study. The CT images were provided by the Teaching Hospital of the University of Chile (Hospital Clínico de la Universidad de Chile, Santiago de Chile) in accordance with their ethics protocol for the use of patient data. The images were obtained using a Siemens 64-channel multidetector CT scanner equipped with a STRATON tube (Siemens Somatom Sensation 64, Siemens Healthcare, Erlangen, Germany) for medical reasons unrelated to this study. The CTs belonged to individuals without skull deformities or orthognatic surgery, and had full or almost-full dentition (i.e., absence of the third molar, occasional loss of 1–2 post-canine teeth). Scans were taken with jaws closed, which is important because this allows landmarking of the cranium and mandible in the knowledge that the dentition is always in or very close to occlusion. It is unlikely that clenching, which could have increased muscle CSA, happened during imaging because patients are asked not to clench as part of the imaging protocol. However, this cannot be ruled out. Due to the medical origin of the CT scans, the coverage of scans differs among patients, with many lacking a complete mandible. The primary reconstruction of images for the purpose of selection of suitable scans was performed using Syngo Multimodality Workplace (Siemens Healthcare, Erlangen, Germany). Voxel sizes ranged from 0.39–0.46 mm × 0.39–0.46 mm × 1 mm (mean size 0.43 mm × 0.43 mm × 1 mm). The image stacks were exported as DICOM files for their use in this study.

Three-dimensional (3D) skull morphologies were reconstructed from the CT stacks using Avizo (v.7.0.1, Visualization Sciences Group, Burlington, USA). Semi-automated segmentation of CTs based on grey-level thresholds to separate bone from surrounding tissues and air was undertaken. Additionally, manual segmentation was performed where needed.

2.1. Muscle CSAs

The procedure to estimate the CSA of masticatory muscles from CT scans was based on Weijs and Hillen (1984), and referred to in a previous study (Toro-Ibacache et al., in press).

2.1.1. Temporalis muscle

In a sample of human cranial MRI scans, Weijs and Hillen (1984) found that the largest temporalis muscle CSAs are found in planes that lie 4–16 mm (with a mean of 10 mm) above and parallel to the Frankfurt plane (defined here between left infraorbital, and left and right portion). For this study, we standarised the sectioning plane to (1) be parallel to the Frankfurt plane, and (2) to pass through the most medial point of the infratemporal crest. The latter is identifiable on all specimens and lies within the region in which Weijs and Hillen (1984) found CSA to vary little (4–16 mm above the Frankfurt plane). Temporalis CSA was estimated as the average of the muscle CSA in this sectioning plane and in two planes (∼1 and 2 mm) immediately above it (Fig. 2).

2.1.2. Masseter and medial pterygoid muscles

Weijs and Hillen (1984) found that the largest CSAs of both muscles to be in a plane inclined about 30° to the Frankfurt plane, 25 mm above the mandibular angle; and that the CSA is largely unchanged in planes ranging between 12 and 30 mm below the zygomatic arch. In our sample, the mandibular angle could not always be used due to its absence in CT scans. However, the lingula was identifiable in all CT stacks and lies within the aforementioned range of distances from the zygomatic over which CSA changes little. We standardised the sectioning plane to be parallel to the infero-posterior border of the zygomatic bone (which is the orientation of the origin of the

Table 1
Landmarks used for shape analysis.

No.	Name	Definition
1	Vertex	Highest point of the cranial vault
2	Nasion	Intersection between frontonasal and internasal junction
3	Anterior nasal spine	Tip of the anterior nasal spine
4	Prosthion	Most buccal and occlusal point of the interalveolar septum between central incisors
5	Occiput	Most posterior point of the skull
6 & 20	Supraorbital torus	Most anterior point of supraorbital ridge
7 & 21	Infraorbitale	Most inferior point of the infraorbital ridge
8 & 22	Nasal notch	Most lateral part of the nasal aperture
9 & 23	First molar	Most buccal and mesial point of the junction of the M1 and the alveolar process. If M1 is absent, the landmark is in the lowest most buccal point of the interalveolar septum between the second premolar and the next molar
10 & 24	Last molar	Most buccal and distal point of the junction between the.last molar and the alveolar process
11 & 25	Zygo-maxillar	Most inferior point of the zygomatico-maxillary junction
12 & 26	Fronto-zygomatic	Most lateral point of the fronto-zygomatic junction
13 & 27	Fronto-temporal angle	Point at the intersection between frontal and temporal processes of the zygomatic bone
14 & 28	Zygomatic arch lateral	Most lateral point of the zygomatic arch
15 & 29	Zygomatic root posterior	Most posterior-superior point of the intersection between the zygomatic root and the squama of the temporal bone
16 & 30	Zygomatic root anterior	Most anterior point of the intersection between the zygomatic root and the squama of the temporal bone
17 & 31	Zygomatic arch medial	Most lateral point on the inner face of the zygomatic arch
18 & 32	Infratemporalis crest	Most medial point of the infratemporal crest
19 & 33	Eurion	Most lateral point of the cranial vault
34 & 38	Coronoid process anterior	Most anterior point of the coronoid process
35 & 39	Coronoid process superior	Most superior point of the coronoid process
36 & 40	Mandibular notch	Most inferior point of the mandibular notch
37 & 41	Condyle	Most lateral point of the condyle
42 & 45	Anterior temporal origin	Most anterior point of origin of the temporal muscle in the temporal line
43 & 46	Superior temporal origin	Most superior point of origin of the temporal muscle in the temporal line
44 & 47	Posterior temporal origin	Most posterior point of origin of the temporal muscle in the temporal line
48 & 51	Anterior masseter origin	Most anterior point of origin of the masseter muscle
49 & 52	Posterior masseter origin	Most posterior point of origin of the masseter muscle
50 & 53	Mid-masseter origin	Midpoint along the area of origin of the masseter muscle
54 & 57	Superior pterygoid origin	Most superior point of the origin of medial pterygoid muscle
55 & 58	Inferior pterygoid origin	Most inferior point of origin of the medial pterygoid muscle
56 & 59	Mid-pterygoid origin	Midpoint along the area of origin of the medial pterygoid muscle

masseter and is found at about 30° to the Frankfurt plane), at the base of the lingula. Masseter and medial pterygoid CSAs were estimated by averaging CSAs from this sectioning plane and two planes that lie ~1 mm above and below it (Fig. 2).

In order to limit errors associated with the definition of muscle contours, the CSA in each section was measured three times and the values averaged, for each of the jaw-elevator muscles. The sectioning and CSA measurements were performed in Avizo.

2.2. Shape analysis

After 3D skull reconstruction, a surface file was generated for each individual and saved as a Wavefront file. Skull geometry was captured using 59 landmarks, described in Table 1 and shown in Fig. 1.

Only the shape of the superior part of the mandibular ramus was represented by landmarks due to the absence of the mandibular body and angle in a large part of the sample. Digitisation of landmarks was performed using the EVAN toolbox (v.1.62, by the European Virtual Anthropology Network-Society www.evan-society.org).

The skull shows a degree of asymmetry, which is irrelevant to this study. It was therefore decided to symmetrise the skulls by reflected relabelling followed by averaging of the original and reflected landmarks (Corti et al., 2001). The symmetrised data were used in subsequent analyses.

Sexual dimorphism in skull shape was assessed using discriminant analysis applied to the shape variables (Procrustes coordinates), using MorphoJ (v.1.06c, Klingenberg, 2011). Reliability was assessed by leave-one-out cross-validation. The permutation test (1000 rounds) showed that this sample is not significantly sexually dimorphic ($p = 0.09$). Thus data are pooled in subsequent shape analyses.

Geometric morphometric analyses of landmark configurations were used to explore patterns of shape variation. These analyses also allowed the identification of individuals with different combinations of facial and neurocranial features, used to test H02. After full Procrustes fit, PCA of shape coordinates was performed to assess overall shape variation in the sample (Mitteroecker and Gunz, 2009; O'Higgins, 2000; Slice, 2007) using the EVAN toolbox.

Hypothesis 1, that there is no association between skull shape and masticatory muscle CSAs, was formally tested using partial-least squares (PLS) and multivariate regression analyses. The PLS method finds pairs of axes, singular warps, for each set (block) of variables through singular value decomposition of the among block covariance matrix (Rohlf and Corti, 2000). Like principal components, the first axis is constructed such that it explains the largest possible proportion of among block covariance with successive orthogonal axes accounting for diminishing proportions (Rohlf and Corti, 2000). Muscle variables correspond to the averaged left and right muscle CSAs of temporalis, masseter, and medial pterygoid. Two sets of PLS analyses were undertaken. In the first, the muscle block of data comprised muscle CSAs and the second, the proportions of total muscle CSA accounted for by each muscle. The first PLS therefore assesses the association between absolute muscle CSAs (and so maximum forces) and skull shape while the second considers relative CSAs and so relative forces by each muscle.

The proportions of covariance explained by the first pairs of singular warps (one being shape, the other muscle data) were computed and correlations between individual scores on them were used as measures of association between the two blocks. Additionally, multivariate regression was used to assess skull and face shape predictability from muscle CSAs or CSA proportions. In addition, the RV coefficient, which is a multivariate generalisation of the squared Pearson correlation coefficient (Escoufier, 1973; Klingenberg, 2009) was used to estimate the strength of

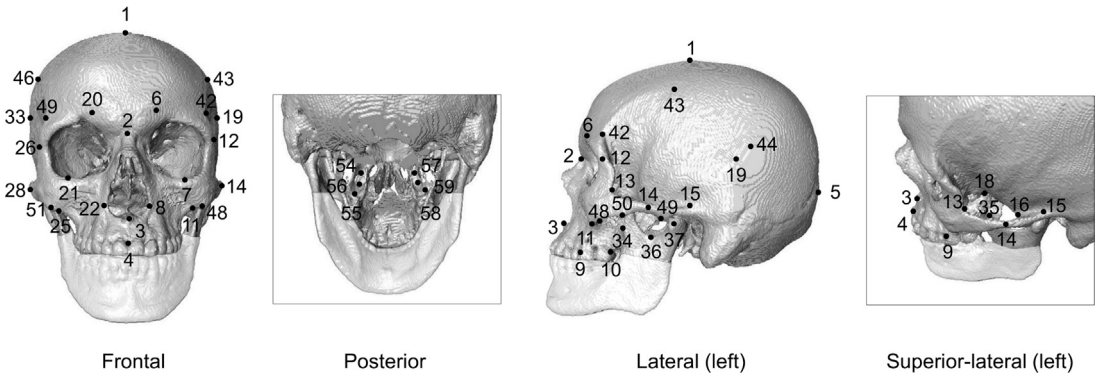

Fig. 1. Selected landmarks listed in Table 1. Landmarks were not placed on the mandibular angle and body due to their absence in most of the sample.

associations among blocks. Permutation tests of 1000 rounds were used to assess statistical significance in all the analyses. The associations between skull shape and muscle data were visualised through surface warpings. These analyses were undertaken using the EVAN toolbox and MorphoJ.

2.3. Finite element analysis

In order to test H02, a subsample of two individuals showing different craniofacial features was selected. These individuals were the most extreme cases on the first principal component of shape and in the PLS of skull shape variables. They differ in the degrees to which their faces and neurocrania are vertically elongated or wide and their degree of maxillary prognathism, variations that are frequently present in human populations (Bhat and Enlow, 1985).

The models were created from the CTs via segmentation as described earlier. The ramus of the mandible was not included in the models. Craniofacial sinuses were preserved and cancellous bone was modelled as cortical, decisions based on the results of prior validation and sensitivity analyses (Fitton et al., 2015; Toro-Ibacache et al., submitted for publication) which showed that omitting cancellous bone decreases model stiffness almost proportionally (i.e., without marked changes in mode of deformation and so, relative strains over the cranium).

The individual with a narrower and more orthognathic maxilla had premature loss of both upper M1s. In order to recreate the proper M1 biting scenario, both M1s were reconstructed by replicating the individual's own upper second molars. The individual with a wider and more prognathic maxilla had premature loss of the upper right first and second premolars, which were reconstructed by mirroring the homologous teeth of the left side. The more orthognathic individual required manual reconstruction of length for both I1s since the CT extended to only to the upper parts of these teeth. After these corrections the volume data were resampled to achieve isometric voxel sizes.

The 3D volumes were exported as BMP stacks and converted by direct voxel-element conversion into meshes of eight-noded cubic elements. Based on literature values and the mentioned

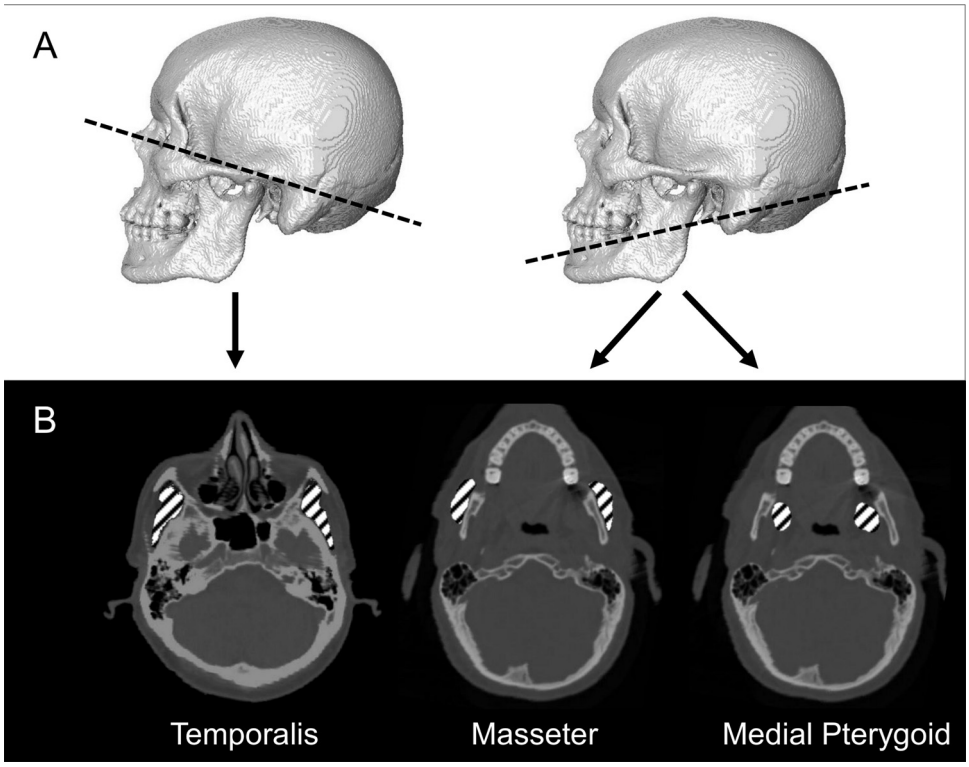

Fig. 2. Cross-sectional areas of jaw-elevator muscles. In (A), orientation of planes for each pair of muscles in (B).

Table 2
Description of FE models. Centroid size based on the landmark configuration in Table 1 minus the mandible landmarks.

Individual	Sex	Age (years)	Centroid size (mm)		CT voxel size (mm)	Number of elements	Temporalis force (*N*)		Masseter force (*N*)		Masseter pterygoid force (*N*)	
			Cranium	Face			Left	Right	Left	Right	Left	Right
Orthognathic	F	54	468.53	218.68	0.45 × 0.45 × 1	7,787,812	195.1	202.2	200.4	227.2	121.4	129.8
Prognathic	M	46	469.36	221.74	0.43 × 0.43 × 1	7,745,806	188.2	194.9	209	225.7	143	153.6

validation study (Toro-Ibacache et al., submitted for publication), a Young's modulus of 17 GPa was assigned to bone (Fitton et al., 2012; Gröning et al., 2011; Kupczik et al., 2009) and of 50 to teeth, the latter being an approximate mean of the large range of values found in the literature for enamel and dentine (Barak et al., 2009; Benazzi et al., 2012; Meredith et al., 1996). Both materials were homogeneously modelled as linearly elastic and isotropic with a Poisson's ratio of 0.3 (Kupczik et al., 2007; Szwedowski et al., 2011). Each model was kinematically constrained at both articular surfaces of the mandibular fossae (simulating a normal human temporomandibular joint) in the *x*, *y* and *z*-axes. Constraints in the vertical axis were placed on the incisal border of both central incisors (I1) and the tip of the four cusps of the left first molar (M1), simulating common human bite points. The characteristics of each model are summarised in Table 2.

Muscle origins and insertions were reproduced in the models based on the original CT images. Maximal jaw-elevator muscle forces per individual were calculated from their CSAs using the equation $F = \text{CSA} \times 37\ \text{N/cm}^2$ where the latter value is an estimate of the intrinsic muscle strength for human masticatory muscles (Koolstra et al., 1988; Weijs and Hillen, 1985). Model pre- and post-processing was performed using the custom, voxel-based FEA software VOX-FE (Fagan et al., 2007; Liu et al., 2012).

Comparison of FEA results was carried out using colour-coded strain contour plots, a qualitative and a quantitative approach aiming to compare the spatial distribution of low and high strains and magnitudes of predicted strains. In order to make models comparable, the strain contour plots of each individual were scaled to represent an I1 bite force of 350 N, and an M1 bite force of 700 N (O'Connor et al., 2005; van Eijden, 1991; Waltimo and Könönen, 1993). This is possible, because the FE models were assigned linearly elastic properties and, with static loads, deformations scale linearly with force. This scaling does not impact on strain distributions, but rather, proportionately on all magnitudes.

3. Results

3.1. Skull shape variation

In the PCAs of skull shape, PC1 and PC2 account for 22.34% and 15.4% = 37.74% of skull shape variance. Thus there is no single strong vector of variation. The male and female distributions overlap almost completely and males appear slightly more variable than females in the plots of Fig. 3. The first two principal components relate to co-variations in both neurocranial and facial proportions (i.e., they are both narrow and tall or wide and long in the insets), and within the face, the maxilla is more or less prognathic (Fig. 3).

3.2. Association between skull shape and jaw-elevator muscle CSAs

Two-block PLS analyses examined the associations between muscle CSAs, proportions of total muscle CSA and skull shape. The CSAs and proportions were entered singly into the analyses as one 'block' of data and the shape coordinates for the sample as the other block. As expected, given that one block contains only one variable, the PLS analyses resulted in one singular value (SV) explaining 100% of the covariance of CSA with skull or face shape. The RV coefficient was also calculated as a measure of association between these blocks.

Temporalis proportion showed the strongest association with skull shape with the correlation among first singular warps (SW1) being the greatest ($r = 0.71$) yet insignificant ($p = 0.44$). The RV coefficient for the skull (RV = 0.21) with temporalis proportion was the largest found, but does not achieve significance. Temporalis proportion also explained the greatest (yet quite small) proportion of the total variance of skull shape ($R^2 = 0.07$; i.e., 7% of the total variance).

Morphologically, SW1 from the PLS of skull shape against temporalis proportion suggests that a large temporalis proportion is associated with a relatively antero-posteriorly elongated neurocranium and mandibular ramus, wider upper face and less prognathic, narrower, vertically shorter maxilla compared to those individuals with small temporalis proportions (Fig. 4). The transformation grids show large deformations of the lateral aspects of the neurocranium. These reflect shifts in the relative positions of the Eurion (most lateral point of the neurocranium), a type 3 landmark (Bookstein, 1991) with respect to the landmarks representing temporalis attachment.

In prior FE-based studies of the primate cranium, it is mostly the face that deforms under simulated biting loads (Fitton et al., 2012; Kupczik et al., 2009; Wroe et al., 2010). Thus, we carried out a second PLS analysis using a subset of 43 facial landmarks (Table 1), to see if the face alone reflects the association between skull shape and muscle parameters (CSAs and their proportions of total CSA). When only the facial landmarks are considered, the results parallel those of the skull, with temporalis proportion showing the strongest association with facial morphology as assessed by the correlation among SW1s ($r = 0.81$), strength of covariation (RV = 0.29), and proportion of total variance explained ($R^2 = 0.09$). Only the relationship between temporalis proportion and face shape was statistically significant at the $p < 0.05$ level (Table 3), but not after Bonferroni correction (corrected p-value 0.05/12 = 0.004). Morphologically, a large temporalis proportion appears to be associated with a relatively narrow, less prognathic, vertically shorter maxilla, relatively wider upper face, and an antero-posteriorly elongated mandibular ramus and a low-set coronoid process when compared to small temporalis proportion (Fig. 5).

3.3. Cranial response to masticatory loading

FEA results show that the distribution (not magnitudes) of regions of high and low strains in the contour plots is very similar between models, irrespective of their general cranial features. High strains are found at the masseter and medial pterygoid insertions, over the skeleton closely related to the biting tooth, the mandibular fossae and, depending on bite location, the compact-bone structures surrounding facial cavities that form the facial buttresses (Donat et al., 1998; Linnau et al., 2003). Thus, the largest strains are located in the face. During I1 bites, relatively large strains are found in regions close to the bite point; the alveolar process, nasal notch, frontal process of the maxilla, mandibular fossa and anterior palate. During M1 bites, strains are similarly greatest in the region of the bite point but the palatal strains are low in both individuals (Fig. 6). The main differences between individuals are found

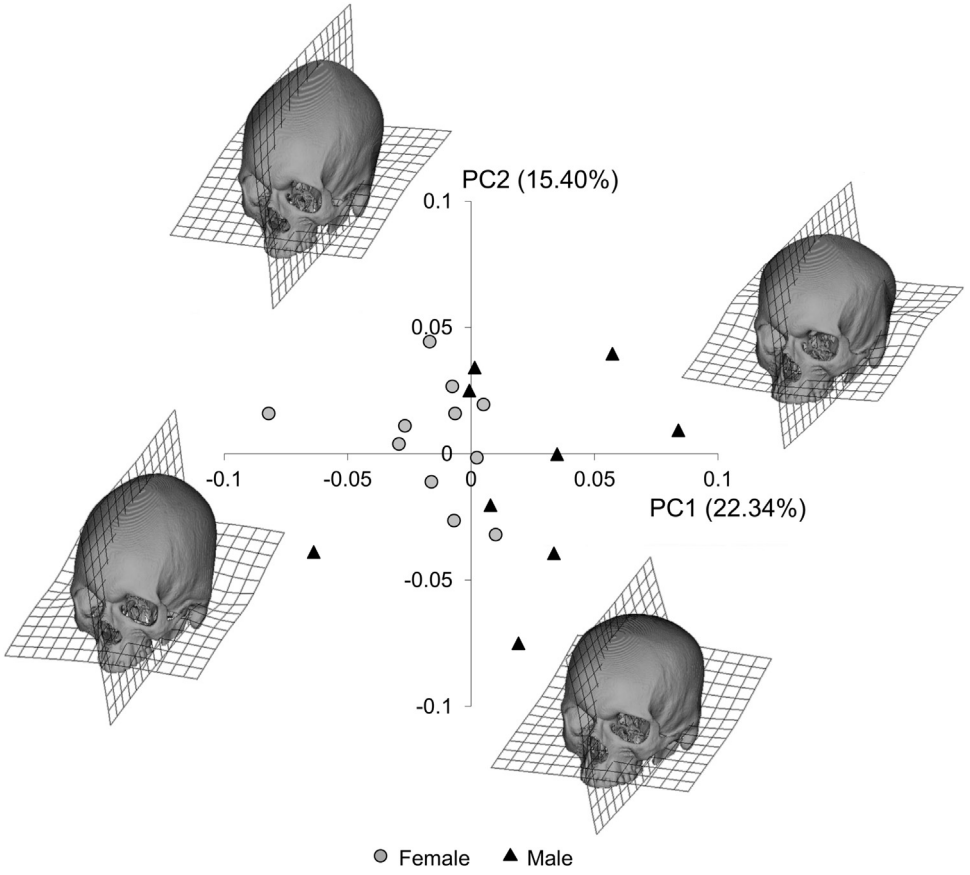

Fig. 3. Principal components analysis of skull shape coordinates. Visualisations of variation represented by each PC are shown as warped surfaces and transformation grids at their positive and negative extremes. Warpings are with respect to the mean and have been magnified 1.5 times to improve visualisation.

Table 3
Relationship between skull and face shape and masticatory muscle CSAs and proportions of total muscle CSA.

Variable	Structure	PLS					Regression	
		SV	Correlation (r)	p-Value	RV	p-Value	R^2	p-Value
Temporalis CSA	Skull	1.11	0.76	0.20	0.16	0.37	0.06	0.37
	Face	1.07	0.67	0.80	0.24	0.07	0.08	0.07
Masseter CSA	Skull	1.23	0.60	0.91	0.11	0.83	0.04	0.83
	Face	1.06	0.76	0.36	0.12	0.77	0.04	0.77
Medial pterygoid CSA	Skull	1.66	0.72	0.38	0.17	0.36	0.06	0.37
	Face	0.98	0.78	0.24	0.18	0.29	0.06	0.29
Temporalis proportion	Skull	0.07	0.71	0.44	0.21	0.13	0.07	0.13
	Face	0.07	0.81	0.12	0.29	0.02	0.09	0.02
Masseter proportion	Skull	0.04	0.61	0.90	0.10	0.86	0.03	0.86
	Face	0.04	0.68	0.76	0.14	0.63	0.05	0.64
Medial pterygoid proportion	Skull	0.06	0.68	0.59	0.17	0.36	0.06	0.35
	Face	0.05	0.71	0.63	0.20	0.20	0.06	0.21

over the maxilla during I1 biting; the orthognathic individual shows markedly lower values of strain (~150 $\mu\varepsilon$) over both vestibular and the palatal aspects of the alveolar process compared to the prognathic individual, in which strains above 250 $\mu\varepsilon$ are present in the same regions (Fig. 6). During molar biting the individuals show a more similar distribution of regions of high strain.

4. Discussion

The present work comprises two complementary studies assessing aspects of the relationship between skull shape and muscle force: (1) the association between skull shape and muscle CSA, and (2) cranial response to biting.

The first study tested the hypothesis that there is no association between skull shape and masticatory muscle CSAs. None of the tested relationships falsified this null hypothesis after Bonferroni correction. Variations in temporalis muscle CSA with facial shape show the strongest association, significant as a single test but not overall. In this regard it should be noted that the sample size is too small to have tested multiple associations between muscle CSAs or proportions and facial form, given that these are unlikely to be of much greater magnitude than we have found. The second study aimed to understand how different skull morphologies, as observed in the first study, differ in their cranial response to biting. We tested the hypothesis that crania with different morphologies show different cranial responses to simulated biting. These findings are further discussed below.

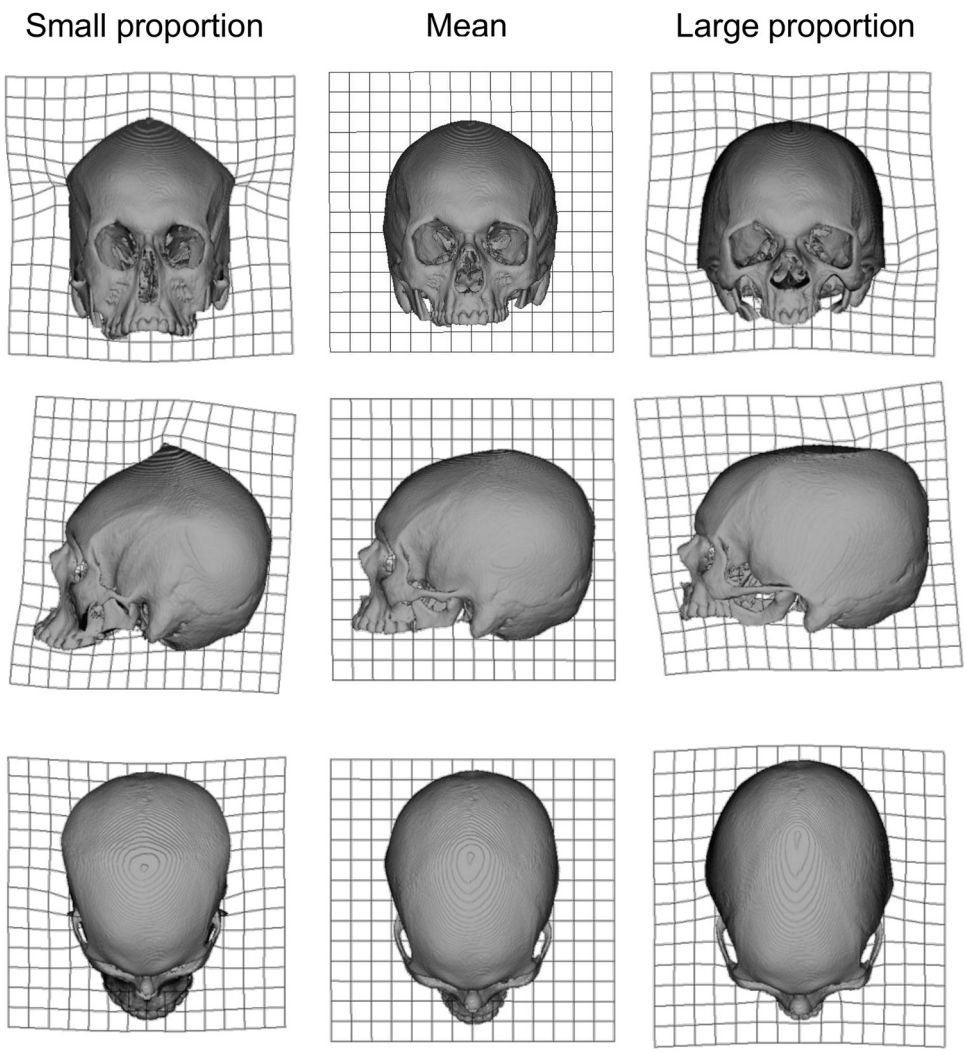

Fig. 4. Association between skull shape and temporalis muscle proportion. Warpings of skull shape on SW1 scores. Individuals with a large temporalis proportion show an antero-posteriorly elongated neurocranium and mandibular ramus and a vertically shorter face. Surface warpings have been magnified three times respect to the mean to improve visualisation.

The first part of the present work failed to show any significant association between skull or facial shape and muscle CSAs or proportional CSAs; despite the significant association for the single test of temporalis proportion, this is not statistically significant after Bonferroni correction for multiple tests (Table 3). As noted above, this may reflect lack of association, but it also could be the result of a small sample size and indicates that a future study should examine a larger sample and test only this association. Despite this, there is evidence of a weak relationship between temporalis muscle CSA and skull and face shape that is at least consistent with the location, anatomy and function of this muscle and anatomical space required to accommodate it. Among jaw-elevators, the temporalis muscle has the largest CSA (Weijs and Hillen, 1984), the longest fibres, the largest PCSA and the largest mass of contractile tissue (van Eijden et al., 1997). A fully activated temporalis muscle or at least as activated as all the jaw-elevators, as it has been reported to happen during both symmetric and asymmetric bites (Spencer, 1998; van Eijden, 1990), has therefore the greatest potential impact on bone morphology. This could occur by producing the highest strains at both the mandibular insertion and bite points. The albeit insignificant association found here between temporalis CSA as a proportion of total masticatory muscle CSA and facial shape, namely the suggestion that large temporalis proportions are associated with a relatively narrower, less prognathic, vertically shorter maxilla and vice versa, is in agreement with previous studies using linear morphometrics. Thus, Weijs and Hillen (1986) have also noted that temporalis and masseter CSA appear to be positively correlated with facial width. With regard to the relationship found between a relatively small temporalis proportion and a vertically elongated skull and face, van Spronsen (2010) noted such an association and suggested that a long face is the result of a diminished muscle force, product of small size and intrinsic strength. The latter would be produced by a high proportion of slow-twitch type I muscle fibres, which produce less strength per unit area than type II fibres.

In individuals with a large temporalis proportion, medio-lateral and antero-posterior enlargement of the inferior opening of the temporal fossa, may provide space for a muscle with a large CSA. The low position of the coronoid process and consequent more vertical orientation of the temporalis have been suggested to increase mechanical efficiency in the human masticatory system (Nicholson and Harvati, 2006). In relation to the relationship suggested by the present analyses between larger temporalis proportion and narrower maxillae, there are few and inconclusive studies addressing the mechanical impact of variations in maxillary width on masticatory mechanics. In women, a wide dental arch has been noted to

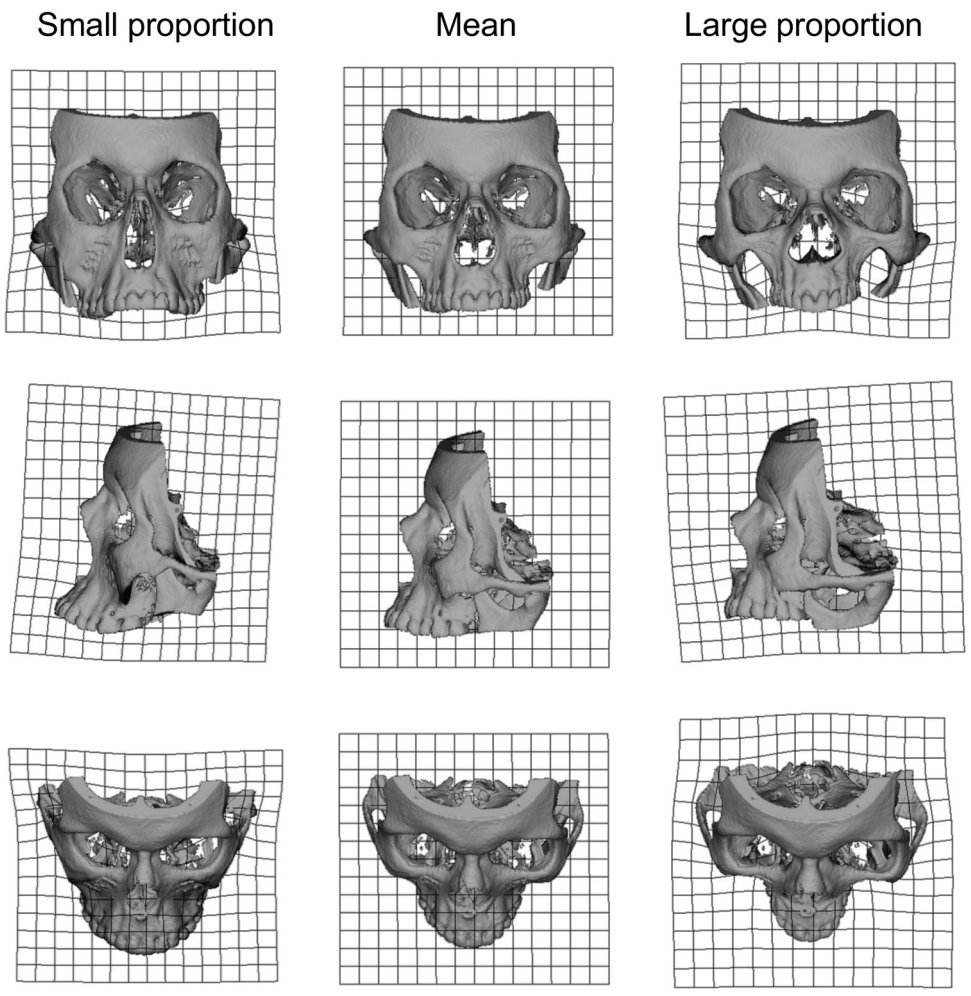

Fig. 5. Association between face shape and temporalis muscle proportion. Warpings of facial shape on SW1 scores. In individuals with large temporalis proportion, the maxilla is narrower and less prognathic than in individuals with a small temporalis proportion. In the mandible, the coronoid process is less prominent and in a low position in individuals with large temporalis proportion. Surface warpings have been magnified three times respect to the mean to improve visualisation.

be associated with a (medio-laterally) thicker masseter (Kiliaridis et al., 2003), whereas no relationship between bite force and dental arch width was found in pre-adolescents (Sonnesen and Bakke, 2005). It should be borne in mind, however, that a combination of an orthognathic, less prognathic and wide maxilla at the posterior teeth (and vice versa) may result in deviations from the normally found elliptic–parabolic (in rough terms) maxillary arch (Burris and Harris, 2000; Ferrario et al., 1994), and therefore a narrow maxilla in individuals with a large temporalis proportion may not necessarily be functionally significant.

As expected, the FEA showed that during both I1 and M1 biting high strains are found at the masseter and medial pterygoid insertions, over the skeleton closely related to the biting tooth, the mandibular fossae and the facial buttresses. These resemble the results of other FEA studies of human and non-human primates (Fitton et al., 2012; Gross et al., 2001; Jansen van Rensburg et al., 2012; Kupczik et al., 2009; Ross et al., 2011; Strait et al., 2009; Szwedowski et al., 2011; Wroe et al., 2010). Despite the differences in morphology, the simulated bites strain both crania similarly in terms of distribution; with strains over these regions varying in magnitude. The exception is found in the maxilla; peak strains over it, particularly the alveolar process and palate, attain significantly lower values in the individual with the narrowest, most vertically oriented maxilla, compared to the more prognathic individual. Since both models have practically the same centroid size (Table 2), these results are not likely to relate to size differences.

Variations in the morphology of the craniofacial skeleton in modern humans have been associated with factors such as population history, geography, climate and diet (Strand Viðarsdóttir et al., 2002; Lieberman, 2008; Noback et al., 2011; Smith, 2011; von Cramon-Taubadel, 2011, 2013). von Cramon-Taubadel (2011) showed that the shape of the mandible is significantly correlated with diet, while the maxilla–palate complex is not when controlling for the effects of population history. Our results suggest that the form of the maxilla could reflect masticatory system loading. Although the association with jaw-elevator muscle forces is weak overall, when the results of the two parts of the present study are considered together they suggest a relationship between the morphology of the maxilla and both the force input and cranial skeletal deformation during biting. Although the nature of this relationship cannot be fully elucidated by our study, it is plausible that the maxilla tends to deform less in individuals with the ability to generate large muscle forces (and hence, large bite forces). This requires further studies with larger samples to better assess the veracity of this association and if shown to be significant, how it arises during ontogeny, if it reflects an ontogenetic adaptation to bite forces. Thus clinical studies have shown that there is a close link between the magnitudes and direction of both occlusal (biting) and muscular forces. Among these, a relationship has been found between occlusal interferences and the production of bruxism (Behr et al., 2012), between the correction of inverted upper–lower molar relationships and mandibular movements during chewing (Piancino

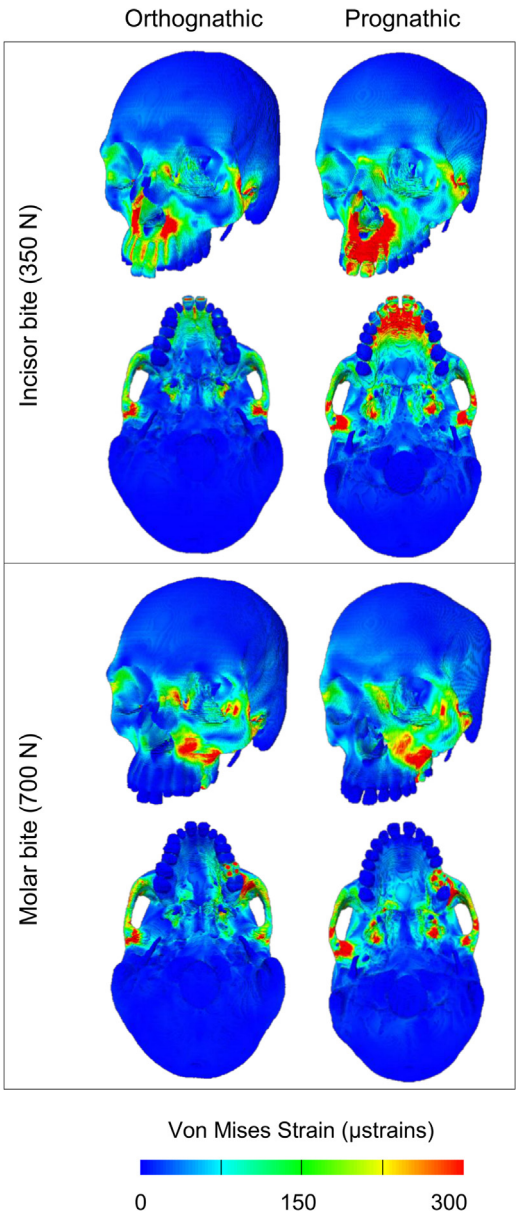

Fig. 6. Von Mises strain contour plots of FE models of crania with different neurocranial and facial morphologies. The strain contour plots represent the cranial response to simulated I1 and M1 bites. The orthognathic individual has a vertically oriented, narrow maxilla compared to the prognathic individual. Size of the models is not scaled.

et al., 2006), and between tooth replacement by implants and the alteration of functional parameters (Meyer et al., 2012). These studies highlight not only the importance of normal occlusal loads in maintaining the functional health of the masticatory system, but also reflect the anatomical, functional, and thus likely ontogenetic links between occlusal forces and masticatory muscle function through the periodontal tissue connecting teeth with the maxilla and the periodontal proprioceptors in it (Behr et al., 2012; Herring, 1985; van Spronsen, 2010).

In conclusion, there is a weak relationship between jaw-elevator muscle force parameters and skull morphology, although there is weak support for an association between temporalis muscle proportion and facial morphology. Among facial structures, the shape of the maxilla has a marked effect on the magnitudes of strains developed over the anterior maxilla during anterior bites; it deforms less in the more orthognathic individual. An orthognathic maxilla is also present in individuals with a large temporalis muscle proportion, suggesting a key role of the form of the maxilla in the production and resistance of masticatory loads. Further studies are needed in order to unravel this relationship.

Acknowledgements

The authors would like to thank the organisers and assistants of the 16th International Symposium on Dental Morphology and 1st Congress of the International Association for Paleodontology where this work was presented. This study was funded by Becas Chile Grant (Comisión Nacional de Investigación Científica y Tecnológica de Chile, Chile) to VT-I.

References

Anderson, P., Renaud, S., Rayfield, E., 2014. Adaptive plasticity in the mouse mandible. BMC Evol. Biol. 14, 85.
Antón, S.C., 1996. Cranial adaptation to a high attrition diet in japanese macaques. Int. J. Primatol. 17, 401–427.
Antón, S.C., 1999. Macaque masseter muscle: internal architecture, fiber length and cross-sectional area. Int. J. Primatol. 20, 441–462.
Barak, M.M., Geiger, S., Chattah, N.L.-T., Shahar, R., Weiner, S., 2009. Enamel dictates whole tooth deformation: a finite element model study validated by a metrology method. J. Struct. Biol. 168, 511–520.
Barak, M.M., Lieberman, D.E., Hublin, J.-J., 2011. A Wolff in sheep's clothing: trabecular bone adaptation in response to changes in joint loading orientation. Bone 49, 1141–1151.
Behr, M., Hahnel, S., Faltermeier, A., Bürgers, R., Kolbeck, C., Handel, G., Proff, P., 2012. The two main theories on dental bruxism. Ann. Anat. 194, 216–219.
Benazzi, S., Kullmer, O., Grosse, I.R., Weber, G.W., 2012. Brief communication: comparing loading scenarios in lower first molar supporting bone structure using 3D finite element analysis. Am. J. Phys. Anthropol. 147, 128–134.
Bhat, M., Enlow, D.H., 1985. Facial variations related to headform type. Angle Orthod. 55, 269–280.
Bookstein, F.L., 1991. Morphometric Tools for Landmark Data: Geometry and Biology. University Press, Cambridge.
Burris, B.G., Harris, E.F., 2000. Maxillary arch size and shape in American blacks and whites. Angle Orthod. 70, 297–302.
Corti, M., Aguilera, M., Capanna, E., 2001. Size and shape changes in the skull accompanying speciation of South American spiny rats (Rodentia: *Proechimys* spp.). J. Zool. 253, 537–547.
Demes, B., 1987. Another look at an old face: Biomechanics of the neandertal facial skeleton reconsidered. J. Hum. Evol. 16, 297–303.
DiGirolamo, D.J., Kiel, D.P., Esser, K.A., 2013. Bone and skeletal muscle: neighbors with close ties. J. Bone Miner. Res. 28, 1509–1518.
Donat, T.L., Endress, C., Mathog, R.H., 1998. Facial fracture classification according to skeletal support mechanisms. Arch. Otolaryngol. Head Neck Surg. 124, 1306.
Dumont, E.R., 1997. Cranial shape in fruit, nectar, and exudate feeders: implications for interpreting the fossil record. Am. J. Phys. Anthropol. 102, 187–202.
Escoufier, Y., 1973. Le traitement des variables vectorielles. Biometrics 29, 751–760.
Fagan, M.J., Curtis, N., Dobson, C.A., Karunanayaje, J.H., Kupczik, K., Moazen, M., Page, L., Phillips, R., O'Higgins, P., 2007. Voxel-based finite analysis – working directly with MicroCT scan data. J. Morphol. 268, 1071.
Ferrario, V.F., Sforza, C., Miani, A., Tartaglia, G., 1994. Mathematical definition of the shape of dental arches in human permanent healthy dentitions. Eur. J. Orhod. 16, 287–294.
Fitton, L., Shi, J., Fagan, M., O'Higgins, P., 2012. Masticatory loadings and cranial deformation in *Macaca fascicularis*: a finite element analysis sensitivity study. J. Anat. 221, 55–68.
Fitton, L.C., Prôa, M., Rowland, C., Toro-Ibacache, V., O'Higgins, P., 2015. The impact of simplifications on the performance of a finite element model of a *Macaca fascicularis* cranium. Anat. Rec. 298, 107–121.
Frost, H.M., 1987. Bone "mass" and the "mechanostat": a proposal. Anat. Rec. 219, 1–9.
Gingerich, P.D., 1979. The human mandible: lever, link, or both? Am. J. Phys. Anthropol. 51, 135–137.
González-José, R., Ramírez-Rozzi, F., Sardi, M., Martínez-Abadías, N., Hernández, M., Pucciarelli, H.M., 2005. Functional–cranial approach to the influence of economic strategy on skull morphology. Am. J. Phys. Anthropol. 128, 757–771.
Gröning, F., Liu, J., Fagan, M.J., O'Higgins, P., 2011. Why do humans have chins? Testing the mechanical significance of modern human symphyseal morphology with finite element analysis. Am. J. Phys. Anthropol. 144, 593–606.
Gross, M.D., Arbel, G., Hershkovitz, I., 2001. Three-dimensional finite element analysis of the facial skeleton on simulated occlusal loading. J. Oral Rehabil. 28, 684–694.
Hannam, A., Wood, W., 1989. Relationships between the size and spatial morphology of human masseter and medial pterygoid muscles, the craniofacial skeleton, and jaw biomechanics. Am. J. Phys. Anthropol. 80, 429–445.
Herring, S.W., 1985. The ontogeny of mammalian mastication. Am. Zool. 25, 339–350.

Hylander, W.L., 1975. The human mandible: lever or link? Am. J. Phys. Anthropol. 43, 227–242.
Jansen van Rensburg, G.J., Wilke, D.N., Kok, S., 2012. Human skull shape and masticatory induced stress: objective comparison through the use of non-rigid registration. Int. J. Numer. Method Biomed. Eng. 28, 170–185.
Kiliaridis, S., Georgiakaki, I., Katsaros, C., 2003. Masseter muscle thickness and maxillary dental arch width. Eur. J. Orhod. 25, 259–263.
Kiliaridis, S., Mejersjö, C., Thilander, B., 1989. Muscle function and craniofacial morphology: a clinical study in patients with myotonic dystrophy. Eur. J. Orhod. 11, 131–138.
Klingenberg, C.P., 2009. Morphometric integration and modularity in configurations of landmarks: tools for evaluating a priori hypotheses. Evol. Dev. 11, 405–421.
Klingenberg, C.P., 2011. MorphoJ: an integrated software package for geometric morphometrics. Mol. Ecol. Resour. 11, 353–357.
Koolstra, J., Tanaka, E., 2009. Tensile stress patterns predicted in the articular disc of the human temporomandibular joint. J. Anat. 215, 411–416.
Koolstra, J., van Eijden, T., Weijs, W., Naeije, M., 1988. A three-dimensional mathematical model of the human masticatory system predicting maximum possible bite forces. J. Biomech. 21, 563–576.
Kupczik, K., Dobson, C.A., Crompton, R.H., Phillips, R., Oxnard, C.E., Fagan, M.J., O'Higgins, P., 2009. Masticatory loading and bone adaptation in the supraorbital torus of developing macaques. Am. J. Phys. Anthropol. 139, 193–203.
Kupczik, K., Dobson, C.A., Fagan, M.J., Crompton, R.H., Oxnard, C.E., O'Higgins, P., 2007. Assessing mechanical function of the zygomatic region in macaques: validation and sensitivity testing of finite element models. J. Anat. 210, 41–53.
Lieberman, D.E., 2008. Speculations about the selective basis for modern human craniofacial form. Evol. Anthropol. 17, 55–68.
Linnau, K.F., Stanley Jr., R.B., Hallam, D.K., Gross, J.A., Mann, F.A., 2003. Imaging of high-energy midfacial trauma: what the surgeon needs to know. Eur. J. Radiol. 48, 17–32.
Liu, J., Shi, J., Fitton, L.C., Phillips, R., O'Higgins, P., Fagan, M.J., 2012. The application of muscle wrapping to voxel-based finite element models of skeletal structures. Biomech. Model. Mech. 11, 35–47.
Macho, G.A., Shimizu, D., Jiang, Y., Spears, I.R., 2005. Australopithecus anamensis: a finite-element approach to studying the functional adaptations of extinct hominins. Anat. Rec. A Discov. Mol. Cell. Evol. Biol. 283A, 310–318.
Menéndez, L., Bernal, V., Novellino, P., Perez, S.I., 2014. Effect of bite force and diet composition on craniofacial diversification of Southern South American human populations. Am. J. Phys. Anthropol. 155, 114–127.
Meredith, N., Sherriff, M., Setchell, D., Swanson, S., 1996. Measurement of the microhardness and Young's modulus of human enamel and dentine using an indentation technique. Arch. Oral Biol. 41, 539–545.
Meyer, G., Fanghänel, J., Proff, P., 2012. Morphofunctional aspects of dental implants. Ann. Anat. 194, 190–194.
Milne, N., O'Higgins, P., 2012. Scaling of form and function in the xenarthran femur: a 100-fold increase in body mass is mitigated by repositioning of the third trochanter. Proc. R. Soc. B 279, 3449–3456.
Mitteroecker, P., Gunz, P., 2009. Advances in geometric morphometrics. Evol. Biol. 36, 235–247.
Moss, M.L., 1962. The functional matrix. In: Vistas in Orthodontics. Lea & Febiger, Philadelphia, pp. 85–98.
Muchlinski, M.N., Deane, A.S., 2014. The interpretive power of infraorbital foramen area in making dietary inferences in extant apes. Anat. Rec. 297, 1377–1384.
Nicholson, E., Harvati, K., 2006. Quantitative analysis of human mandibular shape using three-dimensional geometric morphometrics. Am. J. Phys. Anthropol. 131, 368–383.
Noback, M.L., Harvati, K., Spoor, F., 2011. Climate-related variation of the human nasal cavity. Am. J. Phys. Anthropol. 145, 599–614.
O'Connor, C.F., Franciscus, R.G., Holton, N.E., 2005. Bite force production capability and efficiency in Neandertals and modern humans. Am. J. Phys. Anthropol. 127, 129–151.
O'Higgins, P., 2000. The study of morphological variation in the hominid fossil record: biology, landmarks and geometry. J. Anat. 197, 103–120.
O'Higgins, P., Jones, N., 1998. Facial growth in Cercocebus torquatus: An application of three-dimensional geometric morphometric techniques to the study of morphological variation. J. Anat. 193, 251–272.
Piancino, M.G., Talpone, F., Dalmasso, P., Debernardi, C., Lewin, A., Bracco, P., 2006. Reverse-sequencing chewing patterns before and after treatment of children with a unilateral posterior crossbite. Eur. J. Orhod. 28, 480–484.
Raadsheer, M., van Eijden, T., van Ginkel, F., Prahl-Andersen, B., 1999. Contribution of jaw muscle size and craniofacial morphology to human bite force magnitude. J. Dent. Res. 78, 31–42.
Rohlf, F.J., Corti, M., 2000. Use of two-block partial least-squares to study covariation in shape. Syst. Biol. 49, 740–753.
Rohlf, F.J., Marcus, L.F., 1993. A revolution in morphometrics. Trends Ecol. Evol. 8, 129–132.
Röhrle, O., Pullan, A.J., 2007. Three-dimensional finite element modelling of muscle forces during mastication. J. Biomech. 40, 3363–3372.
Ross, C.F., Berthaume, M.A., Dechow, P.C., Iriarte-Diaz, J., Porro, L.B., Richmond, B.G., Spencer, M., Strait, D., 2011. *In vivo* bone strain and finite-element modeling of the craniofacial haft in catarrhine primates. J. Anat. 218, 112–141.
Ross, C.F., Iriarte-Diaz, J., 2014. What does feeding system morphology tell us about feeding? Evol. Anthropol. 23, 105–120.
Ross, C.F., Metzger, K.A., 2004. Bone strain gradients and optimization in vertebrate skulls. Ann. Anat. 186, 387–396.
Rubin, C.T., Lanyon, L.E., 1985. Regulation of bone mass by mechanical strain magnitude. Calcif. Tissue Int. 37, 411–417.
Scott, J.H., 1957. Muscle growth and function in relation to skeletal morphology. Am. J. Phys. Anthropol. 15, 197–234.
Sellers, W.I., Crompton, R.H., 2004. Using sensitivity analysis to validate the predictions of a biomechanical model of bite forces. Ann. Anat. 186, 89–95.
Slice, D.E., 2007. Geometric morphometrics. Annu. Rev. Anthropol. 36, 261–281.
Smith, H.F., 2011. The role of genetic drift in shaping modern human cranial evolution: a test using microevolutionary modeling. Int. J. Evol. Biol. 2011, 11.
Sonnesen, L., Bakke, M., 2005. Molar bite force in relation to occlusion, craniofacial dimensions, and head posture in pre-orthodontic children. Eur. J. Orhod. 27, 58–63.
Spencer, M.A., 1998. Force production in the primate masticatory system: electromyographic tests of biomechanical hypotheses. J. Hum. Evol. 34, 25–54.
Spencer, M., Demes, B., 1993. Biomechanical analysis of masticatory system configuration in neandertals and inuits. Am. J. Phys. Anthropol. 91, 1–20.
Strait, D.S., Weber, G.W., Neubauer, S., Chalk, J., Richmond, B.G., Lucas, P.W., Spencer, M.A., Schrein, C., Dechow, P.C., Ross, C.F., 2009. The feeding biomechanics and dietary ecology of *Australopithecus africanus*. PNAS 106, 2124–2129.
Strand Viðarsdóttir, U., O'Higgins, P., Stringer, C., 2002. A geometric morphometric study of regional differences in the ontogeny of the modern human facial skeleton. J. Anat. 201, 211–229.
Szwedowski, T.D., Fialkov, J., Whyne, C.M., 2011. Sensitivity analysis of a validated subject-specific finite element model of the human craniofacial skeleton. Proc. Inst. Mech. Eng. H J. Eng. 225, 58–67.
Taylor, A.B., 2006. Feeding behavior, diet, and the functional consequences of jaw form in orangutans, with implications for the evolution of Pongo. J. Hum. Evol. 50, 377–393.
Toro-Ibacache, V., Fitton, L.C., Fagan, M.J., O'Higgins, P. Validation of a voxel-based finite element model of a human cranium using digital speckle interferometry, *J. Anat.* (under review).
Toro-Ibacache, V., Zapata Muñoz, V., O'Higgins, P., 2015b. The predictability from skull morphology of temporalis and masseter muscle cross-sectional areas in humans. Anat. Rec. A Discov. Mol. Cell. Evol. Biol., in press.
van Eijden, T., 1990. Jaw muscle activity in relation to the direction and point of application of bite force. J. Dent. Res. 69, 901–905.
van Eijden, T., 1991. Three-dimensional analyses of human bite-force magnitude and moment. Arch. Oral Biol. 36, 535–539.
van Eijden, T., Korfage, J., Brugman, P., 1997. Architecture of the human jaw-closing and jaw-opening muscles. Anat. Rec. 248, 464–474.
van Spronsen, P., Weijs, W., Valk, J., Prahl-Andersen, B., van Ginkel, F., 1991. Relationships between jaw muscle cross-sections and craniofacial morphology in normal adults, studied with magnetic resonance imaging. Eur. J. Orhod. 13, 351–361.
van Spronsen, P., Weijs, W., Valk, J., Prahl-Andersen, B., van Ginkel, F., 1992. A comparison of jaw muscle cross-sections of long-face and normal adults. J. Dent. Res. 71, 1279.
van Spronsen, P.H., 2010. Long-face craniofacial morphology: cause or effect of weak masticatory musculature? Semin. Orthod. 16, 99–117.
von Cramon-Taubadel, N., 2011. Global human mandibular variation reflects differences in agricultural and hunter–gatherer subsistence strategies. PNAS 108, 19546–19551.
von Cramon-Taubadel, N., 2013. Evolutionary insights into global patterns of human cranial diversity: population history, climatic and dietary effects. J. Anthropol. Sci. 91, 1–36.
Waltimo, A., Könönen, M., 1993. A novel bite force recorder and maximal isometric bite force values for healthy young adults. Eur. J. Oral. Sci. 101, 171–175.
Weijs, W., Hillen, B., 1984. Relationship between the physiological cross-section of the human jaw muscles and their cross-sectional area in computer tomograms. Acta. Anat. 118, 129–138.
Weijs, W., Hillen, B., 1985. Cross-sectional areas and estimated intrinsic strength of the human jaw muscles. Acta Morphol. Neer. Scand. 23, 267–274.
Weijs, W., Hillen, B., 1986. Correlations between the cross-sectional area of the jaw muscles and craniofacial size and shape. Am. J. Phys. Anthropol. 70, 423–431.
Wroe, S., Ferrara, T.L., McHenry, C.R., Curnoe, D., Chamoli, U., 2010. The craniomandibular mechanics of being human. Proc. R. Soc. B 277, 3579–3586.
Yoshikawa, T., Mori, S., Santiesteban, A., Sun, T., Hafstad, E., Chen, J., Burr, D.B., 1994. The effects of muscle fatigue on bone strain. J. Exp. Biol. 188, 217–233.